



Research Article

ISSN : 0975-7384  
CODEN(USA) : JCPRC5

## Research on simulation of rack roll-beating forming based on ABAQUS

Li Yuxi, Li Yan and Yuan Qilong

Faculty of Mechanical and Precision Instrument Engineering, Xi'an University of Technology Xi'an, China

### ABSTRACT

The basic principle of cold roll-beating forming was described, finite element model of rack cold roll-beating was established by ABAQUS, the forming process, equivalent strain and stress were analyzed, at the same time, a path on tooth space section was established and changing trend of stress was analyzed in the path. The forming force of rack roll-beating was analyzed. The preliminary experiment of rack cold roll-beating was carried out, and the experiment and simulation analysis results were compared to verify the validity of the finite element analysis. This research establishes a good basis of the theory and application for rack single-point cumulative forming.

**Key words:** Cold roll-beating; Finite element model; Equivalent strain; Forming force

### INTRODUCTION

In recent years, the precise plastic forming technique has been rapidly developed which has been applied in some industrial production fields, for example, precise hot forging, precise rolling forming, precise cold extrusion forming, fine blanking, precision sheet metal forming, the closed die forging, power spinning, etc.. As a new kind of plastic forming technique, high-speed cold roll-beating technique has some advantages such as low material consumption, low energy consumption, low pollution, high efficiency, good performance of the products, etc., and is given more and attentions, researches on cold roll-beating of involute spline, screw, gear have been gradually achieved [1-4].

The domestic and foreign experts in the field of plastic forming tried to apply the technique of cold roll-beating to the production practice, from the beginning of the roll-beating bar, sheet to the later of the spline shaft, long axis, screw, gear, etc., expanding the application field of cold roll-beating constantly. Swiss Grob Company developed the equipment which can produce spline formed by cold roll-beating [5-7]. Li Yan et al. established screw roll-beating stress wave model, analyzed stress wave propagation velocity and propagation law under different working conditions, and carried out the screw cold roll-beating experiments on the lathe of CA6140, confirmed the feasibility and superiority of screw cold roll-beating processing [8-10]. Cui Fengkui built a mathematic model of the rolling wheel outline, carried out spline cold roll-beating experiments, corrected the mathematic model of the rolling wheel outline which used the effect of regeneration of test artifacts on rolling wheel outline, got to meet the requirements of processing rolling wheel outline, and developed the CAD system of rolling wheel and simulation system of roller grinding [11].

The cutting is mainly used for now in rack processing, which cuts off metal fiber streamline of metal blank itself, causing the fracture of metal fiber. So anti-fatigue strength of rack and gear is reduced, the service life is shorten, bearing capacity is restricted [12]. In this paper, according to the principle of high speed cold roll-beating, rack cold roll-beating finite element model is established in the ABAQUS, in which the rack molding process, stress, strain and roll-beating force are analyzed. Then, the rack cold roll-beating experiments are carried out on self-made equipment, simulation results and experimental results are compared to verify the correctness of the simulation and feasibility of the forming technology.

## 2 THE PRINCIPLE OF COLD ROLL-BEATING FORMING

Cold roll-beating forming depends on the material's intrinsic plasticity, within the chain of relative movement between shaped pieces and forming tools (rolling wheel), at the same time, through the reciprocating motion, the forming tools strikes constantly rotating parts surface with high-speed, forcing the metal of part surface flow to produce plastic deformation, thus a cumulative effect is caused by striking in continuous movement, and eventually the predetermined shape without a mold or restraint is obtained, the basic principle of cold roll-beating is shown in the Fig.1.

As shown in the Fig.1, in the process of cold roll-beating forming, the block blank feeds along the horizontal direction, three rolling wheels fixed around the central axis rotate at high speed. Thus under the beating effect of high-speed rolling wheels, the metal materials on the upper surfaces of the blank produce certain displacement. At the same time, the moment of rolling wheels contact with the body material, the friction effect makes the rolling wheel autobiography exercise around its own axis to ensure the rolling between the blank block and rolling wheels. The central axis of cold rolling rotates a circle, each rolling wheel hits a deformation block according to a preset feeding depth, the final contour shape is formed on a specific block blank.

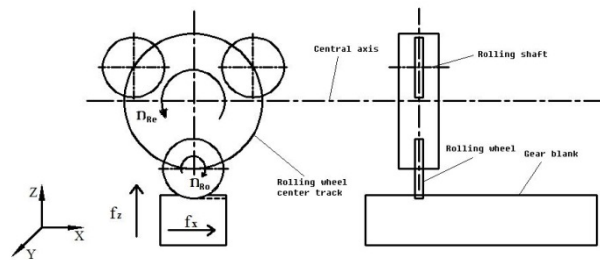


Fig.1 The principle diagram of cold roll-beating forming

## 3 NUMERICAL SIMULATION OF RACK COLD ROLL-BEATING FORMING

### 3.1 The establishment of simulation model

In order to improve the accuracy of finite element simulation and reduce the running time, considering that the bearing shaft of roll-beating equipment have little effect on the simulation results, only rolling wheel and work-piece are established in the simulation model. There are three rolling wheels distributed uniformly on the circus-circle of bearing shaft. Johnson-Cook material model is selected to model the work-piece material which can be expressed as following.

$$\sigma = [A + B\varepsilon^n][1 + C \ln \varepsilon^*][1 - (T^*)^m] \quad (1)$$

Material of the rolling wheel is 40Cr, and the gear billet material is 45# steel. Rolling wheels are constrained as rigid bodies, and are assumed having no deformation in the process of roll-beating, the deformation of work-piece is to be observed. Adding boundary conditions, realizing the rotation of roll-beating equipment in the Y and Z directions, revolutions of three rolling wheels around the X axis, and the forward or backward direction (the Z direction) of the gear billet, the modeling and meshing result is shown in the Fig.2.

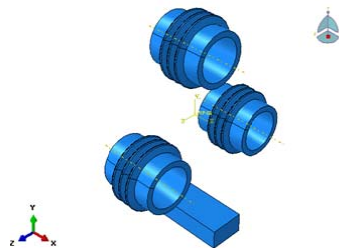


Fig. 2 Geometric model of rack cold roll-beating

### 3.2 Analysis of rack forming process

Fig.3 shows tooth space convex states in different time with simulation parameters of rolling wheel speed 750 rpm, rolling wheel feeding into depth 1mm and the work-piece feeding 60 mm/min. When rolling wheels strike work-pieces, the part of the work-piece is stricken directly by rolling wheel head, due to the continuous radial roll-beating force, bears the biggest force, forming the dedendum. And metal of the both sides is under rolling wheels, bears the extrusion of rolling wheels, and part of the metal flows along the normal direction of the sidewalls

of the rolling wheels to form the sidewall of tooth space, and another part of the metal upward flows along the rolling wheel's sidewall to form a bulge on either side of the tooth space. Then the raised portion flows to the lateral area of smaller resistance, thus the outline shape of tooth space is formed.

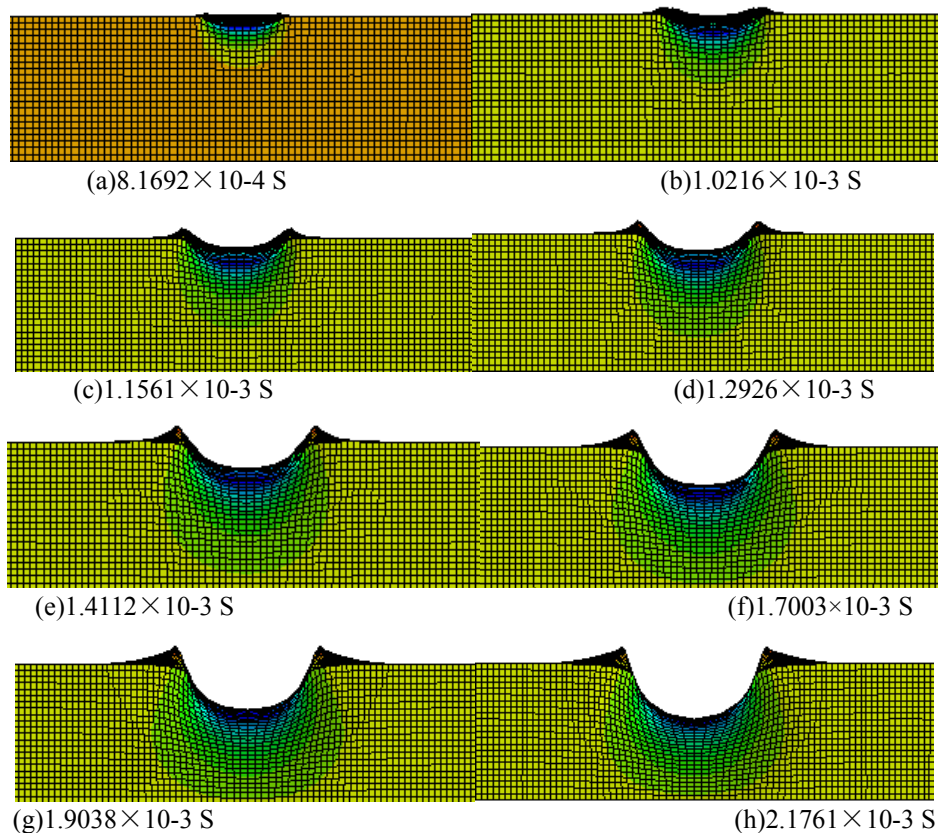


Fig. 3 Contour of tooth space at different moments

### 3.3 Analysis of strain

To analyze the strain of different parts of the tooth space, six meshes on the rack section were taken for strain analysis, as shown in Fig.4 is the distribution of each cell in the position of the tooth space.

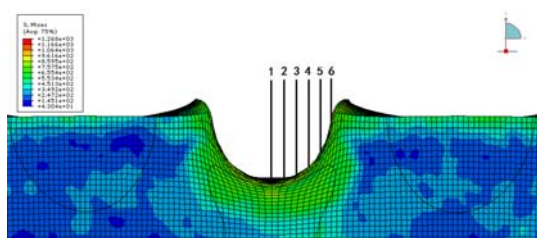


Fig.4 The location of selected elements

The equivalent plastic strain curves of six meshes on the tooth space section in the X direction along with time are shown in the Fig.5. In the X direction, six cells on tooth space, where the stress of cell one, two, three, four, five are of tensile stress types, but six is of compressive stress, six cells in the X direction were stop the deformation after deformation to a certain extent, and plastic strain is a moment of rolling wheel and work-piece contact.

The equivalent plastic strain curves of six cells on the tooth space section in the Y direction along with time are shown in the Fig.6. In the Y direction, six cells on tooth space, where the stress of t mesh one, two, three, four, five are compressive stress, but six is tensile stress, six cells in the Y direction were stop the deformation after deformation to a certain extent, and plastic strain is a moment of rolling wheel and work-piece contact.

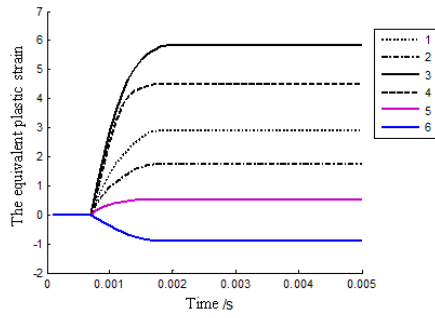


Fig.5 Curves of the equivalent plastic strain of X direction with different time

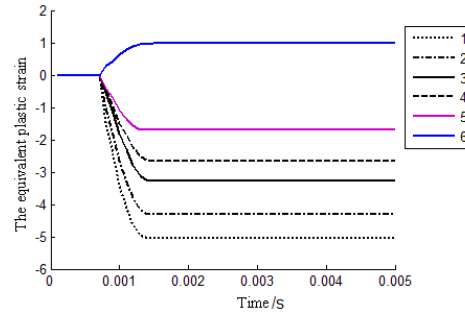


Fig.6 Curves of the equivalent plastic strain of Y direction with different time

Fig.7 shows the equivalent plastic strain curves of the six cells in the shape of tooth slot section-along with the change of time along the Z direction, the cross sections of the alveolar are subjected to compressive stress in the Z direction, because the process of roll-beating, rolling wheel of the tangential force makes the metal flow along the direction of force, so that the grid in the tangential force direction is compressed to generate compressive stress.

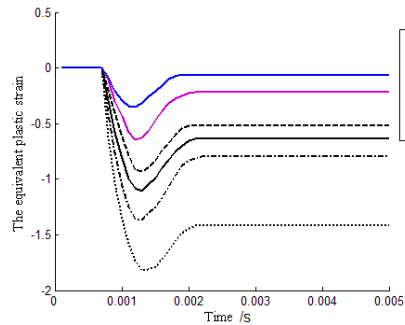


Fig.7 Curves of the equivalent plastic strain of Z direction with different time

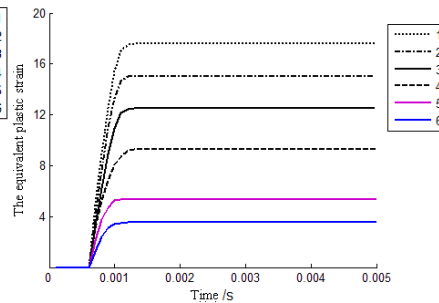


Fig.8 Curves of equivalent plastic strain with different time

Fig.8 shows the total equivalent plastic strain curve of already formed 6 cells. In general, the tooth at the bottom of the cell 1 is a part of the rolling wheel directly struck, so the maximum value of the equivalent plastic strain reached 17.57, the equivalent plastic strain of cell 2 is 15.13, the equivalent plastic strain of cell 3 is 12.53, the equivalent plastic strain of cell 4 is 9.29, the equivalent plastic strain of cell 5 is 5.33, the equivalent plastic strain of cell 6 is 3.56, the equivalent plastic strain values decrease gradually along the tooth slot section upward.

### 3.4 Analysis of stress

The way of cell dividing to analyze the stress at different positions of the tooth space is same as the way of research progress of equivalent plastic strain. As shown in the Fig.4, 6 cells of rack section formed selected to analyze the stress.

The change of the stress with the passage of time curve of 6 cells of the tooth space section formed is shown in the Fig.9. It can be seen from the diagram that the part of biggest stress on work-piece part is dedendum and the part is also the section of largest equivalent plastic strain( cell 1).the stress value at 1050N and the strain values decrease in turn from cell 2 to cell 6 which along the tooth space section upward.

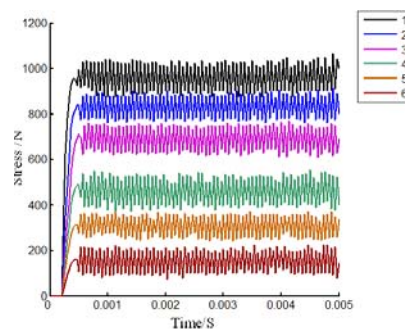


Fig.9Curves of the force of plastic strain with different time

In order to further study the changes of the stress in rolling process, the selected node path is shown in the Fig.10 and analysis the change of stress in this path which is starting from dedendum along the alveolar section up to the top tooth space. The stress variation in the path curve is shown in the Fig.11, which shows the tendency of decrease when along the established path. It consistent with the result of the Fig.9, it is shown in roll-beating process that the biggest stress is dedendum and the stress decreases when along the alveolar wall up gradually.

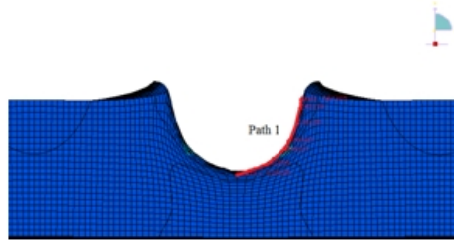


Fig.10 The selection of paths

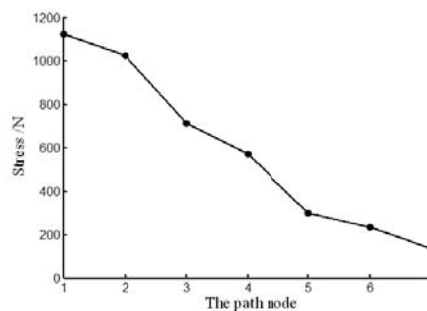


Fig.11 Curves of stress along the path

### 3.5 Analysis of roll-beating force

As shown in the Fig.12, the speed of the rolling wheel for  $n$  (r/min), radius for  $r$ , revolution radius for  $R$ , the time of the rolling wheel setting a single beat on gear billet for  $\Delta t$ , then

$$\Delta t = \frac{60}{n} \times \frac{2\varphi}{2\pi} \quad (2)$$

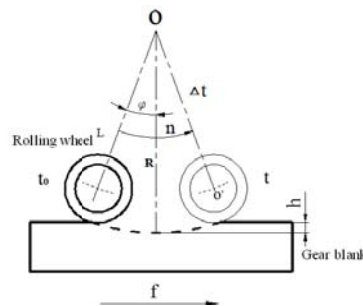


Fig 12 Schematic diagram of cold roll-beating process parameters

Using the model which has been established, while  $n=1180$ r/min, the work-piece feeding amount  $f=60$ mm/min, the amount of beating into  $h=1$ mm, the single roll-beating force curve fig13 of work-piece is got by the simulation .using the equation to calculate that the duration of single cold roll-beating is  $\Delta t=2.825 \times 10^{-3}$ s, in the Fig.13, the simulation results of single cold roll-beating time  $\Delta t=2.8 \times 10^{-3}$ s, so simulation results and calculation results are basically same. It can be seen from the graph, in the stable roll-beating stage, the radial force of the work-piece subjected to be approximately 1250N. Essentially, the cold roll-beating process is a periodic repetition, and the duration of single cold roll-beating is one period. As shown in the Fig.13, it is a period of cold roll- beating .In the Fig.14, the continuous cold roll-beating process is the result of many cumulative periods.



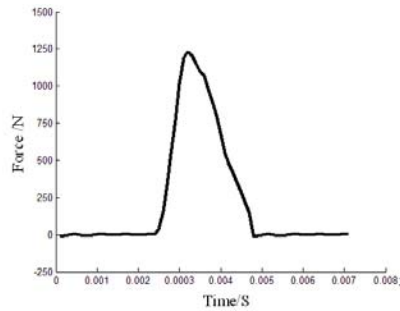


Fig. 13 Radial force graph of single roll-beating

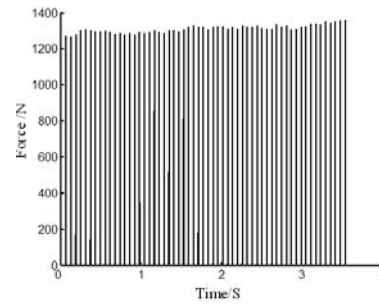


Fig. 14 Radial force graph of Continuous roll-beating

### EXPERIMENTAL SECTION

The experiments are carried out on a horizontal milling machine. The milling cutter is replaced by the specialized rack cold roll-beating equipment. The octagonal ring dynamometer is installed at the bottom of the work-piece. As shown in the Fig. 15, Roll-beating force is measured in the process of cold roll-beating. Through the resistance signal transmission, the strainvalue can be readout on the oscilloscope. According to the static decoupling relationship, the strainvalue can be converted the values of rolling force.

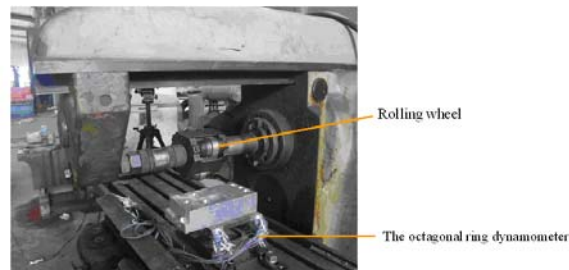


Fig. 15 Roll-beating force measuring device

In experiment process, work-piece materials are duralumin. The rotating speed of the roll-beating wheel is 1180rpm. The feed speed of work-pieces is 60 mm/min. The dynamometer is used by the octagonal ring dynamometer. The data gathering frequency is 500 $\mu$ s. An experimental sample of cold roll-beating is shown in the Fig. 16.



Fig. 16 The test results of hard aluminum cold roll-beating

Fig. 17 shows the force diagram in the initial stage of cold roll-beating. Fig. 17 (a) shows the actual measured axial force in the initial stage of cold roll-beating and Fig. 17 (b) shows the actual measured tangential force in the Initial stage of cold roll-beating. In the inception phase, the axial and tangential forces are gradually increasing. At the beginning of the 4 seconds, the tangential force is greater than the axial force. The tangential force is about 100N and the axial force is less than 50N. But the axial force increases rapidly. When roll-beating process is on to the 6 s, the axial force has been greater than the tangential force and it shows the tendency of increase. Yet, the tangential force increases slowly.

Fig. 18 gives the force diagram in the stabilization stage of cold roll-beating process. Fig. 18(a) shows the actual measured axial force in the Initial stage of cold roll-beating and Fig. 18 (b) shows the actual measured tangential force in the Initial stage of cold roll-beating. In the stable roll-beating stage, the axial force and tangential force value are relatively stable. The axial force keeps about 1380N and the tangential force keeps about 230N. The axial force is greater than the tangential one. The experimental and simulation results are basically identical, which

verifies the rationality and validity of the finite element simulation.

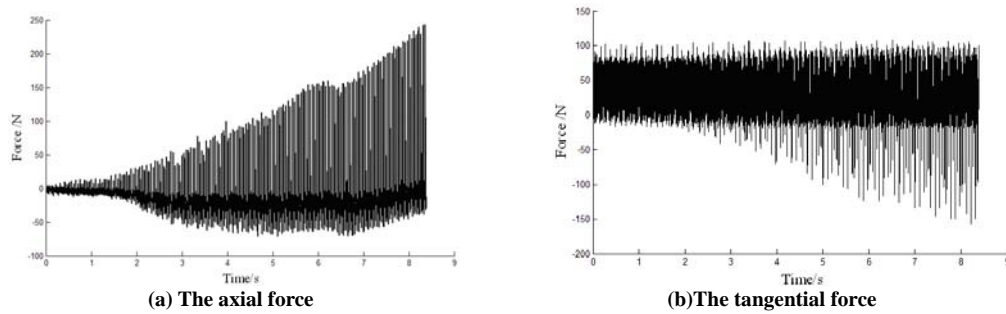


Fig.17 Force graph in the initial stages of cold roll-beating

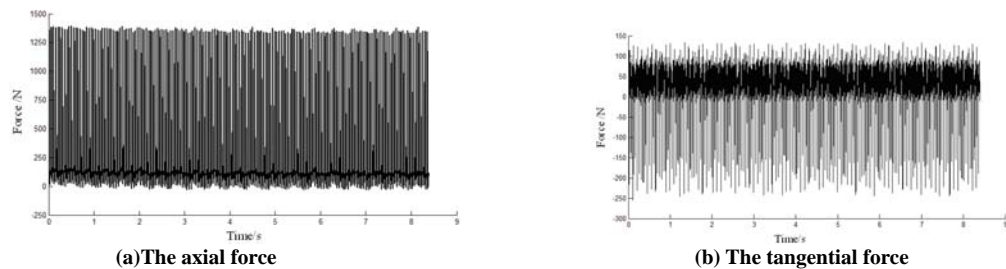


Fig.18 Force graph in the stable stages of cold roll-beating

## CONCLUSION

Finite element model of rack cold roll-beating forming is established by ABAQUS and simulation combined with the actual processing condition is carried out. The forming process of work-piece, the equivalent plastic strain and the stress and stress changing trend on the path are analyzed, and the roll-beating force in the process of roll-beating is analyzed in the simulation. The cold roll-beating experiments are conducted on self-developed experimental equipment. The experimental results match simulation results well, which verifies the validity of the finite element simulation and the feasibility of the rack cold roll-beating. The research results can provide guidance and reference for rack cold roll-beating forming process.

## Acknowledgment

This topic of research is supported by the Natural Science Foundation of China (No. 50975229, 51075124), the Specialized Research Fund for the Doctoral Program of Higher Education of China (No. 20116118110005), Scientific Research Project Plan of Shaan'xi Educational Committee (No. 12JK0688), Key Laboratory of Scientific Research Projects of Shaan'xi Educational Committee (No. 12JS072, 13JS071).

## REFERENCES

- [1] SHAN De-bin, YUAN Lin, GUO Bin. *Journal of Plasticity Gineering*, **2008**, (2):85-86.
- [2] Jeswiet J, Geiger M, Engel U, et al. *CIRP Journal of Manufacturing Science and Technology*, **2008**, 1(1):2-17.
- [3] Amar Kumar Behera, Johan Verbert, Bert Lauwers, Joost R. Duflou. *Computer-Aided Design*, **2013**, 45(3): 575-590.
- [4] R. Neugebauer, K.-D. Bouzakis, B. Denkenac, et al. *CIRP Annals - Manufacturing Technology*, **2011**, 60(2): 627-650.
- [5] Krapfenbauer H. *International Industrial & Production Engineering*, **1984**, 8(3):39-41.
- [6] Krapfenbauer H. *European Production Engineering*, **1994**, 1(9):39-43.
- [7] Silvia Gavliakova, Zuzana Biringero, Jana Plevkova. *Open Journal of Molecular and Integrative Physiology*, **2012**, 02(1): 21-26.
- [8] Zhao Zhiyuan, Yuan Qilong, Yang Mingshun et al. *Foundry Technology*, **2011**, (8): 132-136.
- [9] Li Yan, Zhang Lu, Yang Mingshun, et al. *Key Engineering Materials*, **2011**, 1024(455): 151-155.
- [10] Zhang Lu, Li Yan, Yang Mingshun et al. *China Mechanical Engineering*, **2012**, (8):90-92.
- [11] Han Zhiren, Zhang Fengshou, Cui Fengkui. *Aeronautical Science and Technology*, **2012**, (5): 87-89.
- [12] Ruan Xueyu, Lou Zhenliang. *Die and Mould Technology*, **2003**, (2):4-9.